Chapter 5

Interaction of Sinapic acid with β-casein (milk protein)

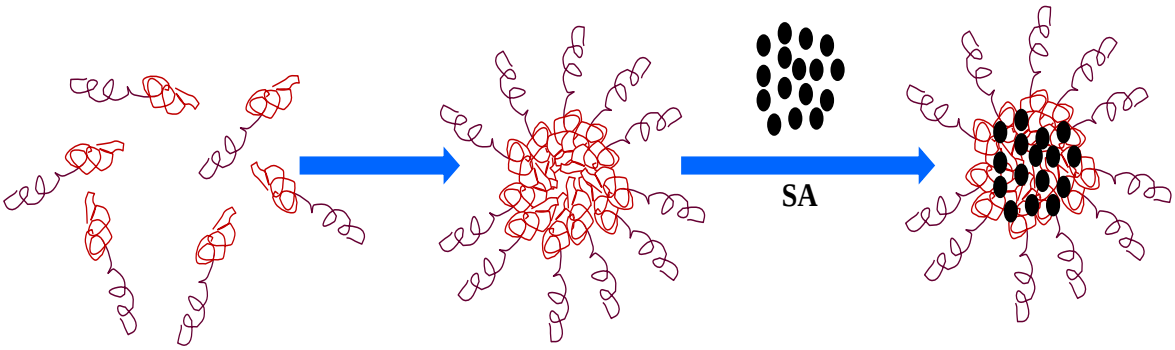

5.1. Introduction

In recent years, adding biologically active natural ingredients to functional food to improve consumer well-being has become increasingly popular. On the other hand, the bulk of these bioactives have low gastrointestinal permeability and poor solubility [Munin et al., 2011; Vieira da Silva et al., 2016]. As a result, many encapsulation technologies have been established to overcome these restrictions and preserve these molecules throughout processing and storage, preserving their active molecular form until they are consumed and delivered to the physiological target within the organism [Okuro et al., 2015; Bahri et al., 2019]. Caseins, a type of mammalian milk protein, have a number of functional properties that make them suitable bioactive carriers [Dalgleish, 2011; Uversky, 2002].

The main component of bovine milk is β-casein. This phosphoprotein has a total of 209 amino acids and a molecular weight of ~24 kDa constitutes about 37% of the caseins in bovine milk and is the most hydrophobic casein [Semo et al., 2007; Shapira et al., 2012]. Due to the separation between its hydrophobic C-terminal domain (rich in proline residues) and its hydrophilic, highly charged N-terminal domain which contains an anionic phosphoserine cluster makes β-casein extremely amphiphilic and allowing it to self-associate in small oblate micelles [Holt et al., 1993; Swaisgood et al., 2003]. Several studies indicate that, at milk pH (6.8) and room temperature, intermolecular interactions create β-casein micelles at concentrations above the critical micellization concentration (CMC) of 0.5-2 mg/mL [Portnaya et al., 2006; Turovsky et al., 2015]. Several researches have looked into encapsulating hydrophobic molecules inside the hydrophobic core of β-casein micelles and found that employing this nanocarrier system, the effectiveness of weakly water-soluble chemicals can be improved [Esmaili et al., 2011; Mehranfar et al., 2013; Bahri et al., 2019]. In this chapter we have explore the interaction between sinapic acid and β-casein.

5.2. Materials and Methods

5.2.1. Materials

Sinapic acid and β-casein from bovine milk (≥98%, molar mass 24 kg/mol) was obtained from Sigma-Aldrich. A stock solution of 5 mM of SA was prepared freshly in 1:4 alcohol:buffer before every experiments. β-casein (β-CN) was dissolved in a 0.1 M sodium phosphate buffer

(PBS), pH 7.0. PBS was made up of 80 mM NaCl, 5.65 mM Na_2HPO_4 and 3.05 mM NaH_2PO_4. The protein concentration was measured spectroscopically at 280 nm using an extinction value of 11,000 M^{-1} cm^{-1} (β-CN, MW = 24,000 g/mol) [Divsalar et al., 2015].

5.2.2 Methods

5.2.2.1. Fluorescence spectroscopy

The fluorescence emission spectra of free β-CN and β-CN-SA were observed in the range 290-500 nm after illumination at 280 nm. The excitation and emission bandwidths were tuned at 10 nm and 5 nm, respectively. The titration was performed by combining a fixed concentration of β-CN (5 mg/ml) with an increasing concentration of SA (0-44 μM) at three different temperatures (203, 308, and 313 K) and allowing it to stand for 5 minutes to equilibrate before beginning each temperature of the experiment.

5.2.2.2. Assay of ROS scavenging activity (DPPH assay)

The DPPH (2, 2-diphenyl-1-picrylhydrazyl) radical scavenging activity was determined according to the method of Xie et al [Xie et al., 2014] with some modifications. The initial stock solution of SA was prepared in alcohol-PBS buffer medium. The required concentration of SA for the assay (60, 70, 80, 90, 100, 150, 200, 250, 300, 350 and 400 μM) was then achieved by further dilution of the stock solutions with PBS buffer. In this method, 0.250 mL of the sample solution (different concentration of SA containing fixed amount 5 mg/mL of β-CN) was added to 1.5 mL of DPPH (0.1 mM) in methanol and mixed well and for comparison with only SA we have taken 0.250 mL of sample solution (different concentration of SA containing fixed amount of only PBS buffer) was added to 1.5 mL of DPPH (0.1 mM) in methanol and mixed well. The solutions were kept in dark for 30 minutes and then absorbance was taken at 517 nm. The below-mentioned equation was utilized to calculate the percentage of scavenging activity:

$$\textbf{Radical Scavenging activity}\ (\%) = \frac{\left(A_{control} - A_{sample}\right)}{A_{control}} \times 100 \qquad (5.1)$$

5.3. Result and Discussion

5.3.1. Fluorescence spectroscopy

A single tryptophan (at position 143 of the amino acid sequence) and several tyrosine residues make up the intrinsic fluorophore of β-CN. The tryptophan residue Trp-143 is located in the surface of the protein [Bourassa et al., 2013]. The milk protein, β-CN elicits strong tryptophan fluorescence at ~340 nm (Fig. 5.1A) in buffer solution after stimulation at 295 nm (where tyrosine absorption is low). The protein excitation at 295 nm generated the emission of mostly tryptophan residues, while the maximal wavelength of free tryptophan emission in buffer solution is close to 352 nm (for human serum albumin) [Pramanik et al., 2021]. A lower λ_{max} of ~340 nm was observed for the single tryptophan of individual β-CN situated in its hydrophobic segment [Bahri et al., 2019; Benzaria et al., 2013]. This blue shift could be related to the residue's a polar environment [Bahri et al., 2019; Benzaria et al., 2013]. The tryptophan fluorescence of β-CN may alter when the small molecules interact with β-CN, depending on the influence of the interaction on the protein structure [Dezhampanah et al., 2017]. It can be seen that the emission spectra of β-CN decreases with increasing concentration of SA. In the presence of SA, the binding of SA to β-CN causes a ~11 nm red shift in the maximum wavelength of fluorescence emission (Fig. 5.1A). This may be attributed to the considerable change in the local environment of the tryptophan residue, which leads to the formation of SA-β-CN complex due to exposed tryptophan [Bahri et al., 2019; Dezhampanah et al., 2017; Mehranfar et al., 2013; Bourassa et al., 2013].

To learn more about the possible quenching mechanisms between phenolic acid and β-CN, temperature-dependent fluorescence spectral measurements were carried out at various temperatures (303, 308, and 313 K), the binding constants were calculated using the fluorescence quenching of β-casein in the presence of SA. Now to determine the existence of static or dynamic quenching in SA and β-CN complexes, Eq. (5.2) was utilised to assess the Stern-Volmer constant [Lakowicz, 2006]:

$$\frac{\mathbf{F_0}}{\mathbf{F}} = \mathbf{1} + \mathbf{K_{SV}}\,[\mathbf{Q}] = \mathbf{1} + \mathbf{k_q} < \boldsymbol{\tau_0} > [\mathbf{Q}] \qquad (\mathbf{5.2})$$

where, F_0 and F are the fluorescence intensities of SA in the absence and presence of SA (quencher), respectively, and [Q] is the concentration of SA. K_{SV} is the Stern-Volmer quenching constant which can be evaluated from the linear relation of F_0/F and [Q]. k_q is the bimolecular quenching rate constant, and $\langle\tau_0\rangle$, the average fluorophore lifetime in the absence of quencher compounds is the order of 10^{-9} s. The Stern-Volmer plots for β-CN quenching by SA at three different temperatures are represented in Fig. 5.1B and the corresponding K_{SV} values are accumulated in Table 5.1. The two bioactive compounds showed a strong linear relationship when the concentration of SA is less than 20 µM, indicating that the quenching is mostly static with some dynamic quenching at high SA concentrations [Bahri et al., 2019]. Using the K_{SV} values the bimolecular quenching constant (k_q) at three temperatures are found to be the order of 10^{13} $M^{-1}s^{-1}$ (Table 5.1). As evident from Table 5.1, a steady decrease of K_{SV} values with increasing temperature convincingly suggested the presence of static quenching in the operative quenching mechanism. For dynamic quenching mechanism the maximum threshold collision quenching constant is $2x10^{10}$ $M^{-1}s^{-1}$ [Lakowicz, 2006]. As we can see from Table 5.1, k_q values are somewhat higher than the diffusion controlled quenching constants supports the occurring of mostly static quenching process.

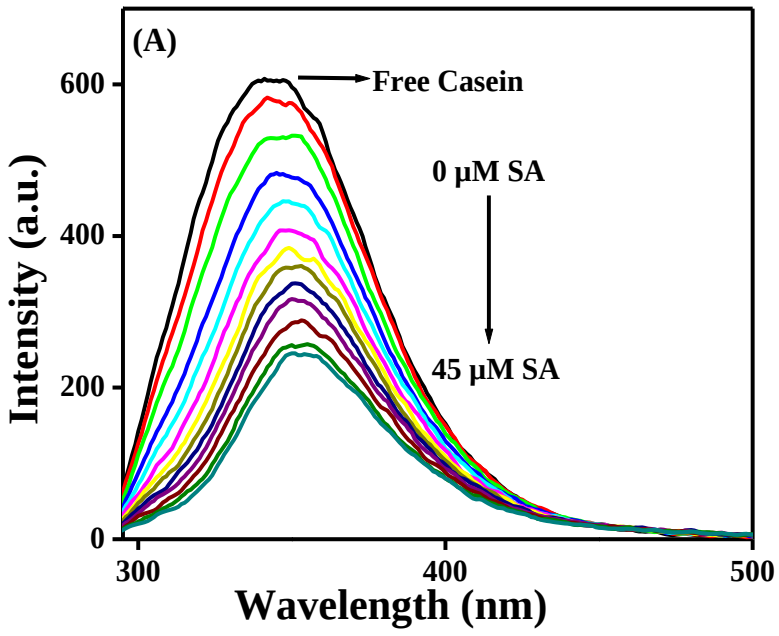

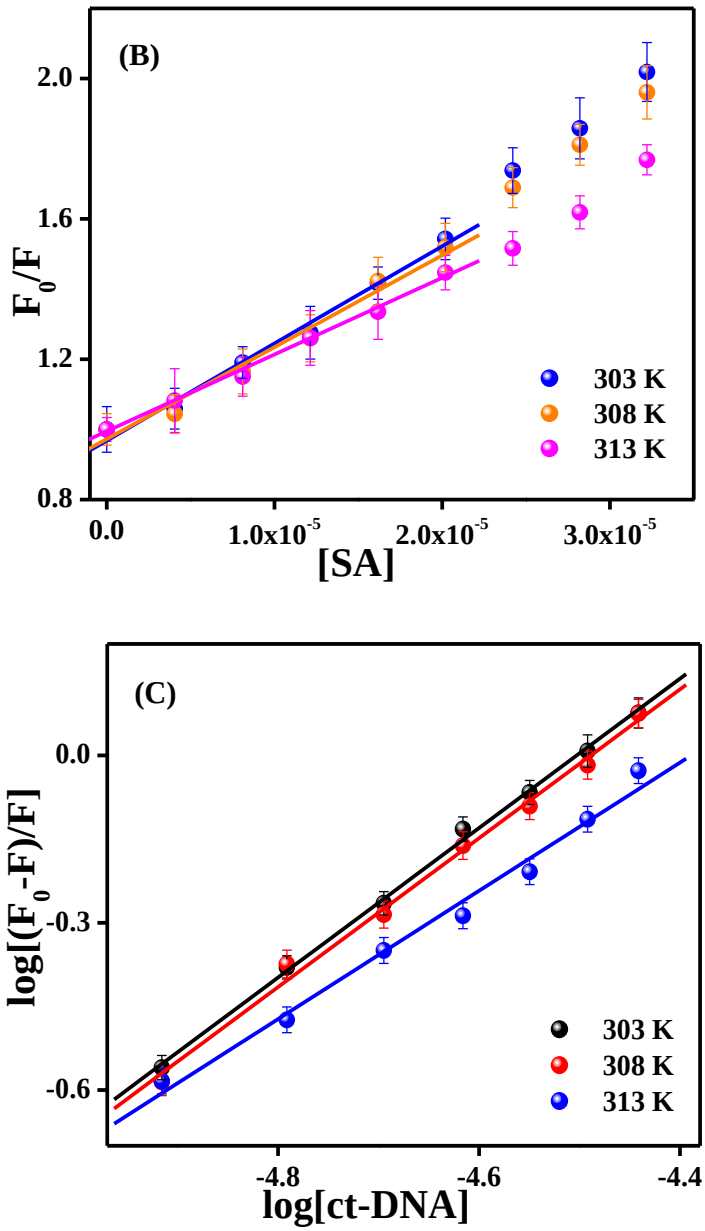

Figure 5.1. (A) The emission spectrum of β-CN by SA, (B) Stern-Volmer plots of the fluorescence quenching of the β-CN by SA and (C) for the binding parameter evaluation with β-CN at three different temperatures

Table 5.1. Variation of Stern-Volmer quenching constant (K_{SV}) and biomolecular quenchin constant (k_q) and modified Stern-Volmer quenching constant at three different temperatures for β-CN-SA system

System	Temperature (K)	K_{SV} (x $10^4 M^{-1}$)	k_q (M^{-1} s^{-1})	R^2
β-CN-SA	303	2.7 ± 0.07	2.77 x 10^{13}	0.9908
	308	2.6 ± 0.01	2.61 x 10^{13}	0.9787
	313	2.1 ± 0.08	2.18 x 10^{13}	0.9962

When small molecules are bound independently to a set of analogous sites on a macromolecule, the binding constant and number of binding sites can be calculated, assuming static quenching according to Eq. (5.3) [Lakowicz, 2006]:

$$\log\frac{(F_0 - F)}{F} = \log K_b + n\log[Q] \qquad (5.3)$$

where, K_b and n are binding constant and the number of binding sites respectively. The value of K_b and n can be obtained from the intercept and slope of the plot log [(F_0-F)/F] vs. log [Q]. The values of K_b and n are listed in Table 5.2. A gradual decrease in K_b value with increasing temperature pointed towards the destabilization of the complex at a higher temperature (Fig. 5.1C). The interaction of SA with β-CN possessed a stronger binding affinities and form 1:1 complex. These findings imply that the phenolic OH groups of SA play a crucial role in the interaction with β-casein [Bahri et al., 2019].

Thermodynamic parameters are essential for predicting the type of contact forces in the interaction of small molecule with β-CN. SA and β-CN can interact in a variety of ways, including hydrogen bonding, hydrophobic forces, van der Waals forces, and electrostatic interactions. Based on the values of entropy change (S) and enthalpy change (H), Ross and Subramanian [Ross et al., 1981] classify interacting forces as follows:

ΔH<0, ΔS<0: van der Waals interaction and hydrogen bond formation.

ΔH>0, ΔS>0: hydrophobic interaction.

ΔH<0, ΔS>0: electrostatic interaction.

The values of free energy change (ΔG), entropy change (ΔS) and enthalpy change (ΔH) were analyzed using the following van't Hoff equation (equation 5.4) [Lakowicz, 2006]:

$$\mathbf{log K_b = -\frac{\Delta H}{RT} + \frac{\Delta S}{R}} \qquad (\mathbf{5.4})$$

$$\mathbf{\Delta G = \Delta H + T\Delta S} \qquad (\mathbf{5.5})$$

where, R is the universal gas constant (8.314 kJ K^{-1} mol^{-1}) and T is the temperature (in Kelvin). The van't Hoff plot is shown in Fig. 5.2A and 5.2B. ΔH and ΔS values were calculated using the slope and intercept of the $\ln K_b$ vs. 1/T plot, respectively. Table 5.2 contains data for all of the thermodynamic parameters for the interaction of β-CN with SA. The binding of SA to β-CN is also an exothermic reaction, although the entropy value is negative. This mechanism is clearly enthalpically driven rather than entropically driven. Both ΔH and ΔS have negative values, indicating that hydrogen bonds and van der Waals forces are important in the creation of the SA-β-CN complex [Dezhampanah et al., 2017]. These interactions may be able to take place via the SA molecule's OH groups and aromatic rings. These results suggest that the SA stabilizes secondary structure of protein [Dezhampanah et al., 2017]. The negative sign for ΔG indicated the spontaneity of the binding process between SA and β-CN.

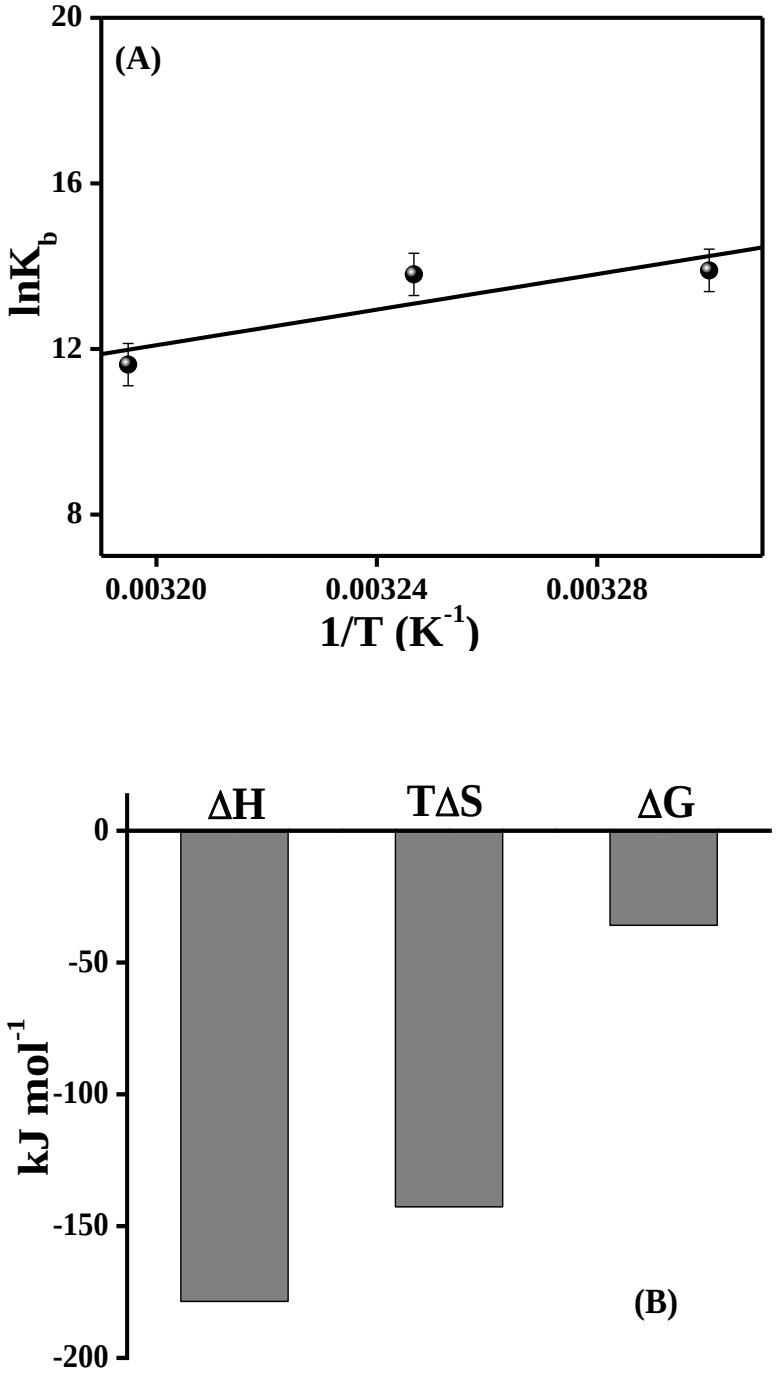

Figure 5.2. van't Hoff plot at three different temperatures for binding of β-CN-SA system (A) and bar diagram plot to visualize the thermodynamic parameters of SA and β-CN (B)

Table 5.2. The binding constant and other thermodynamic parameters for the β-CN-SA system are listed below for three different temperatures

System	Temperature (K)	k_b ($x10^5 M^{-1}$)	n	R^2	ΔH (kJ mol^{-1})	ΔS (J mol^{-1} K^{-1})	ΔG (kJ mol^{-1})
β-CN-SA	303	11.4 ± 0.08	1.34 ± 0.04	0.9976	-178.56	-470.8717	-35.89
	308	9.7 ± 0.07	1.33 ± 0.03	0.9944			-33.53
	313	1.0 ± 0.09	1.14 ± 0.04	0.9870			-31.18

5.3.2. Radical scavenging experiment

Free radical scavenging activity of SA-buffer and SA-β-CN system has been studied by DPPH assay. The SA-β-CN system has a higher DPPH radical scavenging activity than the SA-buffer system. The gradual increase in SA concentration increases the free radical scavenging activity of SA in a dose-dependent manner, which is also significant in the case of the SA-β-CN system. The 200 µM of SA displayed the best result for SA-β-CN system (vide Fig. 5.3).

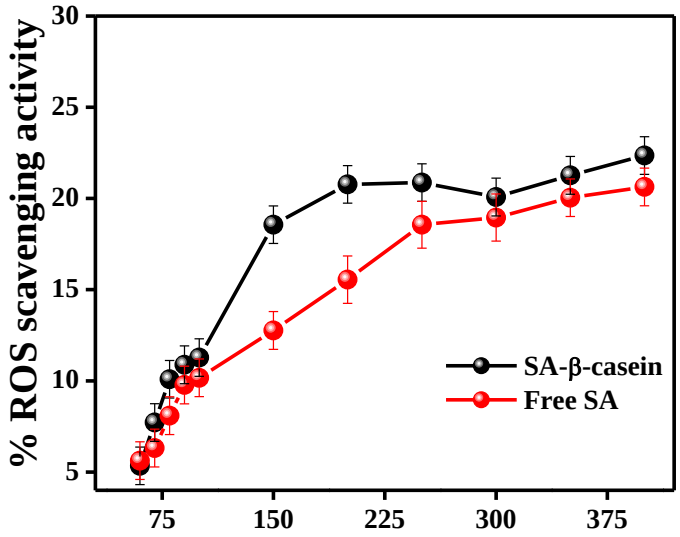

Figure 5.3. ROS scavenging activity of SA in presence and absence of β-CN was measured by DPPH activity

5.4. Conclusion

The present work demonstrates the interaction between milk derived macromolecular protein (β-CN) with SA via various analytical tools. On the basis of spectroscopic results, SA binds with β-CN shows strong binding affinities as well as involvement of hydrogen bonds and van der Waals forces play an important role in the creation of complex between them. Finally, SA-β-CN system shows the greater antioxidant properties than SA. As it is our ongoing work, our next task is to observe the biological efficacy of SA-β-CN and SA system.

5.5. References

Bahri, A., Henriquet, C., Pugnière, M., Marchesseau, S., Chevalier-Lucia, D., 2019. Binding analysis between monomeric β-casein and hydrophobic bioactive compounds investigated by surface plasmon resonance and fluorescence spectroscopy. Food chemistry. 286, 289-296.

Benzaria, A., Maresca, M., Taieb, N., Dumay, E., 2013. Interaction of curcumin with phosphocasein micelles processed or not by dynamic high pressure. Food Chemistry. 138, 2327-2337.

Semo, E., Kesselman, E., Danino, D., Livney, Y. D., 2007. Casein micelle as a natural nano-capsular vehicle for nutraceuticals. Food Hydrocolloids. 21, 936-942.

Bourassa, P., Bariyanga, J., Tajmir-Riahi, H.A., 2013. Binding sites of resveratrol, genistein, and curcumin with milk α-and β-caseins. The Journal of Physical Chemistry B. 117, 1287-1295.

Dalgleish, D.G., 2011. On the structural models of bovine casein micelles-review and possible improvements. Soft matter. 7, 2265-2272.

Dezhampanah, H., Esmaili, M., Khorshidi, A., 2017. Milk β-casein as a vehicle for delivery of bis (indolyl) methane: Spectroscopy and molecular docking studies. Journal of Molecular Structure. 1136, 50-58.

Divsalar, A., Razmi, M., Saboury, A., Mansouri-Torshizi, H., Ahmad, F., 2015. Biological evaluation of a new synthesized Pt (II) complex by cytotoxic and spectroscopic studies. Cell biochemistry and biophysics. 71, 1415-1424.

Esmaili, M., Ghaffari, S. M., Moosavi-Movahedi, Z., Atri, M. S., Sharifizadeh, A., Farhadi, M., Moosavi-Movahedi, A. A., 2011. β-casein-micelle as a nano vehicle for solubility enhancement of curcumin; food industry application. LWT-Food Science and Technology. 44, 2166-2172.

Holt, C., Sawyer, L., 1993. Caseins as rheomorphic proteins: Interpretation of primary and secondary structures of the αs1-, β- and κ-caseins. Journal of the Chemical Society Faraday Transactions. 89, 2683-2692.

Lakowicz; J. R. Principles of Fluorescence Spectroscopy, 3rd ed.; Plenum: New York, 2006. 270-350.

Mehranfar, F., Bordbar, A. K., Fani, N., Keyhanfar, M., 2013. Binding analysis for interaction of diacetylcurcumin with β-casein nanoparticles by using fluorescence spectroscopy and molecular docking calculations. Spectrochimica Acta Part A: Molecular and Biomolecular Spectroscopy. 115, 629-635.

Munin, A., Edwards-Lévy, F., 2011. Encapsulation of natural polyphenolic compounds; a review. Pharmaceutics. 3, 793-829.

Okuro, P. K., Furtado, G. F., Sato, A. C., Cunha, R. L., 2015. Structures design for protection and vehiculation of bioactives. Current Opinion in Food Science. 5, 67-75.

Portnaya, I., Cogan, U., Livney, Y.D., Ramon, O., Shimoni, K., Rosenberg, M., Danino, D., 2006. Micellization of bovine β-casein studied by isothermal titration microcalorimetry and cryogenic transmission electron microscopy. Journal of agricultural and food chemistry. 54, 5555-5561.

Pramanik, U., Chakraborty, S., Bhattacharyya, K., Mukherjee, S., 2021. An intrinsically disordered protein in F127 hydrogel: Fluorescence correlation spectroscopy and structural diversity of beta casein. Chemical Physics Letters. 762, 138105-138113.

Ross, P.D., Subramanian, S., 1981. Thermodynamics of protein association reactions: forces contributing to stability. Biochemistry. 20, 3096-3102.

Shapira, A., Davidson, I., Avni, N., Assaraf, Y. G., Livney, Y. D., 2012. β-Casein nanoparticle-based oral drug delivery system for potential treatment of gastric carcinoma: Stability, target-activated release and cytotoxicity. European Journal of Pharmaceutics and Biopharmaceutics. 80, 298-305.

Swaisgood, H. E. 2003. Chemistry of the caseins. In: P. F. Fox & P. L. H. McSweeney (Eds.), Advanced Dairy Chemistry (Vol. 1, 139-202). New York.

Turovsky, T., Khalfin, R., Kababya, S., Schmidt, A., Barenholz, Y., Danino, D., 2015. Celecoxib encapsulation in β-casein micelles: structure, interactions, and conformation. Langmuir. 31, 7183-7192.

Uversky, V.N., 2002. Natively unfolded proteins: a point where biology waits for physics. Protein science. 11, 739-756.

Vieira da Silva, B., Barreira, J. C. M., Oliveira, M. B. P. P., 2016. Natural phytochemicals and probiotics as bioactive ingredients for functional foods: Extraction, biochemistry and protected-delivery technologies. Trends in Food Science and Technology. 50, 144-158.

Xie, J., Schaich, K.M., 2014. Re-evaluation of the 2,2-Diphenyl-1-picrylhydrazyl Free Radical (DPPH) Assay for Antioxidant Activity. Journal of agricultural and food chemistry, 62, 4251-4260.